Diffusion-Based Clock Synchronization for Molecular Communication under Inverse Gaussian Distribution

Lin Lin, Chengfeng Yang, Maode Ma, Shiwei Ma

***Abstract*—Nanonetworks are expected to expand the capabilities of individual nanomachines by allowing them to cooperate and share information by molecular communication. The information molecules are released by the transmitter nanomachine and diffuse across the aqueous channel as a Brownian motion holding the feature of a strong random movement with a large propagation delay. In order to ensure an effective real-time cooperation, it is necessary to keep the clock synchronized among the nanomachines in the nanonetwork. This paper proposes a model on a two-way message exchange mechanism with the molecular propagation delay based on the inverse Gaussian distribution. The clock offset and clock skew are estimated by the maximum likelihood estimation (MLE). Simulation results by MATLAB show that the mean square errors (MSE) of the estimated clock offsets and clock skews can be reduced and converge with a number of rounds of message exchanges. The comparison of the proposed scheme with a clock synchronization method based on symmetrical propagation delay demonstrates that our proposed scheme can achieve a better performance in terms of accuracy.**

***Keywords*—molecular communication, clock synchronization, inverse Gaussian distribution, maximum likelihood estimation.**

I. INTRODUCTION

NANONETWORKS have emerged as an interesting and important research hot spot in the last few years. Molecular communication in nanonetworks is a novel inter-disciplinary communication methodology at nanoscale [1, 2], combining with nanotechnology, biology and communication technologies. It has an extensive research prospect in the applications of biomedical engineering, environmental monitoring, industrial production and military [1]. Due to the constraints of the scale, the nanomachines can only perform some simple tasks, such as sensing, computing, data storing, or actuation. In order to achieve complex operation, most of the applications require collaborative execution in a distributed manner in the nanonetworks. Some applications such as data fusion, power management and transmission scheduling require all the nanomachines running on an identical time frame [3].

Since a nanonetwork consists of many nanoscale devices running on their own clocks, it is necessary to make these different clocks synchronized. Due to the unique properties of the nanonetworks, the methodologies of clock synchronization proposed for conventional communication networks (e.g., wireless sensor networks) cannot be directly applied to the molecular communication networks: References [4] and [5] have proposed an averaging algorithm for the clock offset compensation for the clock synchronization of wireless sensor networks. However, the design has ignored the propagation delay of information exchange between the sensor nodes. Since in the nanonetworks, the information molecules propagate much more slowly than the electromagnetic wave, the propagation delay is much larger which cannot be ignored in the algorithm design for the clock synchronization. The timing-sync protocol for sensor networks (TPSN) [6] and the recursive time synchronization protocol (RTSP) [7] for wireless sensor networks have considered the propagation delay in the design. However, they have assumed that the propagation delays are bi-directionally symmetrical. While in molecular communication, the molecules move with strong randomness. The assumption of the symmetrical propagation delays is not appropriate for the molecular communication. Reference [8] has proposed a clock synchronization algorithm, named RoATS, based on [4]. The random bounded communication delay has been taken into account and no symmetrical delay is required. The analysis of the propagation delay from the statistical point of view can provide additional information for the clock synchronization. References [9] and [10] have modeled the random propagation delays following the exponential distribution and the Gaussian distribution, respectively. But in the molecular communication, the propagation delays are assumed to follow the inverse Gaussian distribution [11]. This assumption has been verified by [12]. So proper clock synchronization techniques for the molecular communication in nanonetworks are highly demanded.

The specific implementation of the clock synchronization in the nanonetworks has rarely been discussed in the previous research work. It is always assumed that the clocks among the nanomachines are perfectly synchronized [11, 13-15]. In [16] and [3], the concept of the clock of the nanomachines and the clock synchronization among nanomachines have been coined. For the oscillating clock generation in the nanomachine, [17] has proposed a kind of circadian clock. But the requirements of the working environment of the nanomachines limit its usage. In [18] and [19], the authors have proposed using the transcription and translation in the gene expression to form a feedback loop. By this way the oscillation is generated. A molecular phase locked loop (PLL) has also been proposed in [20] for regulating the clock. For the clock synchronization

among nanomachines, in [21] and [22], the authors have used a bacterial quorum sensing mechanism to synchronize clock among nanomachines in the nanonetworks. Molecules, called the inductors, are released by one nanomachine to trigger another nanomachine to release the same self-inductivity molecules. When the concentration of the inductor particles in the environment reaches a certain threshold at a moment, the entire nanonetwork achieves the clock synchronization. In [23] and [24], the clock synchronization has been realized by inhibitory molecules which are released by one transmitter to inhibit the release of the similar molecules from another nanomachine in the nanonetworks. When the concentration of the molecules falls below a certain threshold, those molecules can be released again. The release pulse of the inhibitory molecules can be called a clock synchronization pattern among the nanomachines. The above-mentioned works try to synchronize the oscillation period rather than timing. It is crucial and indispensable for the nanomachines to synchronize their clocks in various applications over the nanonetworks. In [25], the authors have proposed a blind algorithm for the synchronization using non-decision directed maximum likelihood. The clock sequence is calculated by the receiver based on the analysis of the molecular channel delay. Firstly, the authors have introduced the concept of the clock of the nanomachines without illustrating the way to obtain it. Secondly, the authors have designed the sampling sequences of the receiver without a further discussion on they way to synchronize the clock between the transmitter and the receiver.

In this paper, we study the molecular propagation delay, which follows the inverse Gaussian distribution. Based on a mathematical model of a two-way message exchange mechanism, our proposed synchronization scheme uses the inverse Gaussian distribution to derive the relationship among the clock offset, the clock skew and the recorded time stamps. Then, the clock offset and the clock skew are estimated by the maximum likelihood estimation (MLE). The major contributions of this paper are:

a) Modeling the two-way message exchange mechanism with the molecular propagation delay based on an inverse Gaussian distribution.
b) Deriving the estimators of the clock offset and the clock skew by the MLE for the clock synchronization. The closed-form solutions are obtained with the observed time stamps.

The rest of this paper is organized as follows. The overview of the molecular communication system and the statistical molecular propagation delay model are presented in Section II. In Section III, the estimation of the clock offset and the clock skew are discussed by using a two-way message exchange mechanism and the maximum likelihood estimation. The simulation results are presented in Section IV. Section V concludes this paper.

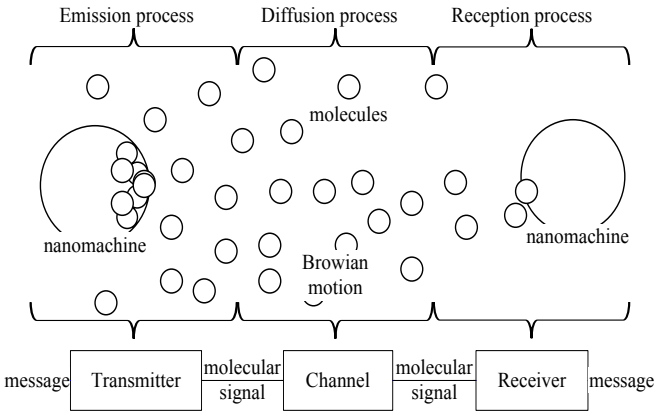

Fig. 1. A point-to-point molecular communication system.

II. Overview of Molecular Communication System and Delay Model

In this section, an overview of the molecular communication system has been described. Then the statistical propagation delay model is presented and explained.

A. Molecular Communication System

Bio-inspired molecular communication is a promising communication paradigm for nanonetworks. It is a kind of short-range communication technology and takes place in aqueous medium which uses chemical or biological molecules as the information carriers. In a point-to-point molecular communication system, a transmitter nanomachine senses a trigger signal and releases the modulated information molecules into a fluid channel. Those molecules propagate to a receiver nanomachine. The receiver senses and receives the information molecules, and operates for the demodulation. The entire molecular communication process consists of emission, diffusion and reception as shown in Fig. 1. The models of the emission process and the diffusion process are described on the basis of the molecular-diffusion physics [26], and the reception process model is interpreted by the theory of the ligand-receptor binding [27]. The molecular communication between the nanomachines is substantially different from the conventional wired or wireless communications.

The complexity of the molecular communication system comes from the Brownian motion of the information molecules and the corrupting noise. In this paper, we consider a scenario where the information molecule propagation takes place inside a space of the fluid medium, which is homogeneous. It is assumed that over the communication process, every information particle is an independent object having identical properties with respect to their shapes and sizes that can be released, diffused, or collected. These assumptions have been made in [13, 21, 28] to study the physical end-to-end model, information capacity and synchronization issues. The information is modulated based on the type of the molecules. Each molecule can carry multiple bits (e.g. n-ary IMoSK proposed in [29]) so that the time stamp message can be encoded into the individual molecule.

B. Statistical Model of the Propagation Delay

In the propagation process, the information molecules diffuse from the transmitter nanomachine to the receiver nanomachine. Since the diffusion of the molecules is governed by the Brownian motion [26, 30], it incurs a propagation delay. Normally, the Gaussian distribution is used to estimate the distance of the Brownian motion within a fixed period in an envisaged scenario of the molecular communication system. The inverse Gaussian distribution is used to describe the distribution of the duration a Brownian motion takes to reach a fixed positive distance [12].

The inverse Gaussian distribution is a continuous probability distribution of two parameters with support on $t \in (0, \infty)$ and it can be used to describe the molecular propagation delay for the information particles arriving at a nanomachine receiver. The probability density function of the molecular propagation delay can be expressed as

$$f(t;\mu;\lambda) = \left(\frac{\lambda}{2\pi t^3}\right)^{\frac{1}{2}} exp\left[-\frac{\lambda(t-\mu)^2}{2\mu^2 t}\right] \quad (1)$$

where $\mu > 0$ is the mean, $\lambda > 0$ is the scaling parameter, t is the propagation delay. μ and λ are dependent on the diffusion coefficient, fluid velocity and the propagation distance. The inverse Gaussian distribution is denoted as $\mathrm{IG}(\mu, \lambda)$.

III. Proposed Maximum Likelihood Estimation

The objective of modeling the diffusion-based clock synchronization for molecular communication is to estimate the clock offset and the clock skew. The clock offset describes a time difference between two nodes. The clock skew is a phenomenon, in which a clock does not run at the exactly same speed as the reference clock. It is caused by the clock accuracy as well as ambient effects such as temperature, pressure and aqueous medium. We consider a two-way message exchange mechanism between two nanomachines, which is mentioned in the clock synchronization protocols for conventional networks such as NTP [31] and TPSN [6].

A reference node (R) and its child node (C) with imperfect clocks are considered. The time stamps of the two-way message exchanges are collected for achieving the clock synchronization as shown in Fig. 2. In the i th round of the message exchange, node R sends a synchronization message command to node C at $T_{1,i}$. Node C records its time stamp $T_{2,i}$ at the time instant of the reception of that message, and responds node R at $T_{3,i}$. Node R records the reception time instant of node C's reply as time stamp $T_{4,i}$. After N rounds of message exchanges, node R obtains a set of time stamps $\{T_{1.i}, T_{2,i}, T_{3,i}, T_{4,i}\}_{i=1}^{N}$. For an asymmetric propagation scenario, the mathematical model of the clock synchronization using time stamps, clock skew, clock offset, fixed delay and random delay can be expressed by (2) and (3).

$$T_{2,i} = \theta + \beta\left(T_{1,i} + d + x_i\right) \quad (2)$$

$$T_{3,i} = \theta + \beta\left(T_{4,i} - d - y_i\right) \quad (3)$$

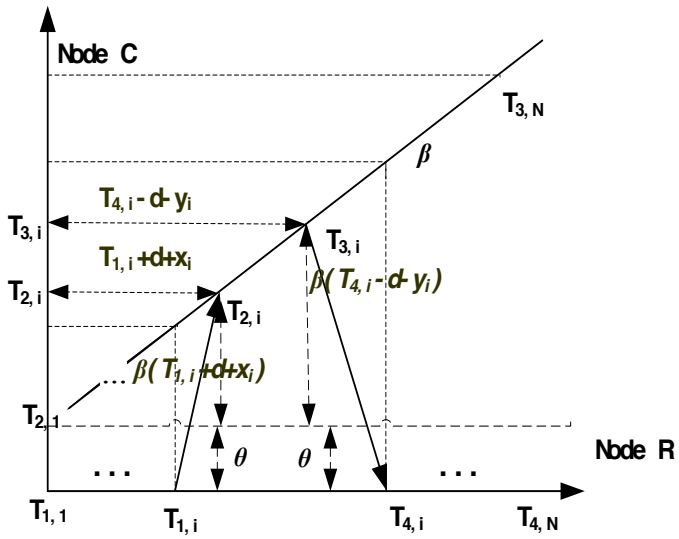

Fig. 2. Two-way time stamps message exchange mechanism.

where θ and β represent the clock offset and the clock skew of the reference node R with respect to its child node C. d stands for the fixed molecular propagation delay from one node to another. It is a non-negative constant related to the molecular propagation distance. x_i and y_i are random molecular propagation delay, where i is a continuous integer from 0 to N. They are modeled as independent identical distributed inverse Gaussian random variables. The work of clock synchronization is to estimate the clock offset θ and the clock skew β based on a set of observations $\{T_{1.i}, T_{2,i}, T_{3,i}, T_{4,i}\}_{i=1}^{N}$.

For clarity, we rewrite (2) and (3) to express the random delays as

$$x_i = \frac{1}{\beta}\left(T_{2,i} - \theta\right) - T_{1,i} - d \quad (4)$$

$$y_i = T_{4,i} - d - \frac{1}{\beta}\left(T_{3,i} - \theta\right) \quad (5)$$

The probability density functions of $\{x_i, y_i\}_{i=1}^{N}$ are given as $\{f(x_i), f(y_i)\}_{i=1}^{N}$. The likelihood function of $\{T_{1.i}, T_{2,i}, T_{3,i}, T_{4,i}\}_{i=1}^{N}$ is given by $\prod_{i=1}^{N} f(x_i) f(y_i)$, where N is the number of rounds of message exchange.

Substitute (4) and (5) into the probability density function of the molecular propagation delay in (1), we can get

$$f\left(\{T_{1,i}, T_{2,i}, T_{3,i}, T_{4,i}\}_{i=1}^{N}, \beta', \theta, d, \mu, \lambda\right) =$$
$$\left(\frac{\lambda}{2\pi}\right)^{N} \prod_{i=1}^{N} \left(\left(\beta'\left(T_{2,i} - \theta\right) - T_{1,i} - d\right)\left(T_{4,i} - d - \beta'\left(T_{3,i} - \theta\right)\right)\right)^{-\frac{3}{2}}$$
$$\times \prod_{i=1}^{N} exp\left(-\frac{\lambda}{2\mu^2}\left(\frac{\left(\beta'\left(T_{2,i}-\theta\right)-T_{1,i}-d-\mu\right)^2}{\beta'\left(T_{2,i}-\theta\right)-T_{1,i}-d} + \frac{\left(T_{4,i}-d-\beta'\left(T_{3,i}-\theta\right)-\mu\right)^2}{T_{4,i}-d-\beta'\left(T_{3,i}-\theta\right)}\right)\right)$$
$$\times I\left(min\left(\beta'\left(T_{2,i} - \theta\right) - T_{1,i} - d\right) \geq 0\right)$$
$$\times I\left(min\left(T_{4,i} - d - \beta'\left(T_{3,i} - \theta\right)\right) \geq 0\right) \quad (6)$$

where $\beta' = \frac{1}{\beta}$ and $I[\cdot]$ is the indicator function. The logarithm of $f\left(\{T_{1,i}, T_{2,i}, T_{3,i}, T_{4,i}\}_{i=1}^{N}, \beta', \theta, d, \mu, \lambda\right)$ can be expressed as

$$L(\beta',\theta,d,\mu,\lambda)=ln\,f\left(\{T_{1,i},T_{2,i},T_{3,i},T_{4,i}\}_{i=1}^{N},\beta',\theta,d,\mu,\lambda\right)=nln\left(\frac{\lambda}{2\pi}\right)$$
$$-\frac{3}{2}\sum_{i=1}^{N}\left(ln\left(\beta'\left(T_{2,i}-\theta\right)-T_{1,i}-d\right)+ln\left(T_{4,i}-d-\beta'\left(T_{3,i}-\theta\right)\right)\right)$$
$$-\frac{\lambda}{2\mu^2}\sum_{i=1}^{N}\left(\frac{\left(\beta'\left(T_{2,i}-\theta\right)-T_{1,i}-d-\mu\right)^2}{\beta'\left(T_{2,i}-\theta\right)-T_{1,i}-d}+\frac{\left(T_{4,i}-d-\beta'\left(T_{3,i}-\theta\right)-\mu\right)^2}{T_{4,i}-d-\beta'\left(T_{3,i}-\theta\right)}\right) \quad (7)$$

The scheme for the clock synchronization consists of two main steps: 1) the estimation for the unknown nuisance parameters μ,λ,d, and 2) the estimation for the clock offset θ and the clock skew β. The second step is directly related to the reliability and stability of the clock.

A Estimation of the Parameters μ,λ,d

The mean μ is used to measure the central tendency of the random variable characterized by the inverse Gaussian distribution. It can be estimated as the average of $\{x_i\}_{i=1}^{N}$ and $\{y_i\}_{i=1}^{N}$ [32].

$$\hat{\mu}=\frac{x_1+x_2+\cdots+x_N+y_1+y_2+\cdots+y_N}{2N}=\frac{\sum_{i=1}^{N}(x_i+y_i)}{2N} \quad (8)$$

Putting (4) and (5) into (8), we have

$$\hat{\mu}=\frac{\sum_{i=1}^{N}(\beta'(T_{2,i}-T_{3,i})+(T_{4,i}-T_{1,i})-2d)}{2N} \quad (9)$$

Considering β',θ,d,μ as fixed parameters, the conditional MLE of λ can be obtained by differentiating the logarithm of (7) with respect to λ and setting the result to zero. The scaling parameter λ can be calculated as

$$\hat{\lambda}=\frac{4N\pi\mu^2}{\sum_{i=1}^{N}\left[\frac{\left[\beta'\left(T_{2,i}-\theta\right)-T_{1,i}-d-\mu\right]^2}{\beta'\left(T_{2,i}-\theta\right)-T_{1,i}-d}+\frac{\left[T_{4,i}-d-\beta'\left(T_{3,i}-\theta\right)-\mu\right]^2}{T_{4,i}-d-\beta'\left(T_{3,i}-\theta\right)}\right]} \quad (10)$$

Putting $\hat{\lambda}$ back into (6), the profile likelihood function becomes

$$f\left(\{T_{1,i},T_{2,i},T_{3,,i},T_{4,i}\}_{i=1}^{N},\beta',\theta,\mathrm{d}\right)=$$
$$\left(\frac{\frac{2N\mu^2}{e^{2\pi}}}{\sum_{i=1}^{N}\left[\frac{\left[\beta'\left(T_{2,i}-\theta\right)-T_{1,i}-d-\mu\right]^2}{\beta'\left(T_{2,i}-\theta\right)-T_{1,i}-d}+\frac{\left[T_{4,i}-d-\beta'\left(T_{3,i}-\theta\right)-\mu\right]^2}{T_{4,i}-d-\beta'\left(T_{3,i}-\theta\right)}\right]}\right)^{N}\times$$
$$\left(\frac{1}{\prod_{i=1}^{N}\left[\left(\beta'\left(T_{2,i}-\theta\right)-T_{1,i}-d\right)\left(T_{4,i}-d-\beta'\left(T_{3,i}-\theta\right)\right)\right]}\right)^{\frac{3}{2}}\times$$
$$I\left(min\left(\beta'\left(T_{2,i}-\theta\right)-T_{1,i}-d\right)\geq 0\right)\times$$
$$I\left(min\left(T_{4,i}-d-\beta'\left(T_{3,i}-\theta\right)\right)\geq 0\right) \quad (11)$$

The MLE is equivalent to maximizing the profile likelihood function [33]. We can derive mathematical expressions of the estimated parameters β',θ,d (denoted as $\hat{\beta}',\hat{\theta},\hat{d}$) by maximizing likelihood function. The MLE that maximizes (11) is equivalent to the solution of the following expression.

$$\left[\hat{\beta}',\hat{\theta},\hat{d}\right]=argmin\sum_{i=1}^{N}\left[\beta'\left(T_{2,i}-T_{3,i}\right)+\left(T_{4,i}-T_{1,i}\right)-2(d+\mu)\right] \quad (12)$$

When $\beta'\left(T_{2,i}-T_{3,i}\right)+\left(T_{4,i}-T_{1,i}\right)-2(d+\mu)=0$, the likelihood function achieves maximum. Using (11) and (12), we can define a feasible region in geometry for unknown parameters β',θ and d.

The propagation of information molecules is a dynamic stochastic process and $x_i\geq 0,\ y_i\geq 0$. We have

$$\beta'\left(T_{2,i}-\theta\right)-T_{1,i}-d\geq 0 \quad (13)$$

$$T_{4,i}-d-\beta'\left(T_{3,i}-\theta\right)\geq 0 \quad (14)$$

For N rounds of message exchanges, the expressions can be presented as

$$\left\{\beta'\left(T_{2,i}-\theta\right)-T_{1,i}-d\geq 0\right\}_{i=1}^{N} \quad (15)$$

$$\left\{T_{4,i}-d-\beta'\left(T_{3,i}-\theta\right)\geq 0\right\}_{i=1}^{N} \quad (16)$$

The fixed delay d can be estimated by calculating the indicator function of the joint maximum likelihood function.

$$\begin{cases}0<\hat{d}\leq\frac{T_{2,i}-\theta}{\beta}-T_{1,i}\\ 0<\hat{d}\leq T_{4,i}-\frac{T_{3,i}-\theta}{\beta}\end{cases},\ i=1,2,\ldots,N \quad (17)$$

The time stamps $\{T_{1,i},T_{2,i},T_{3,i},T_{4,i}\}_{i=1}^{N}$ can be recorded by the two-way message exchange between the node R and the node C. If the fixed delay d is known, the feasible region of the clock offset θ and the clock skew β will be estimated by a set of observed time stamps. The fixed propagation delay will be discussed in Section IV.

B Joint Maximum Likelihood Estimation of the Clock Offset θ and the Clock Skew β

The clock offset and the clock skew can also be estimated by the joint MLE. $\{x_i,y_i\}_{i=1}^{N}$ follows the independent identical distributed inverse Gaussian distribution. The mean $\hat{\mu}$, the scaling parameter $\hat{\lambda}$ and the fixed propagation delay $\hat{d}$ are estimated in Section III(A). Then the clock offset and the clock skew can be estimated by solving a system of equations, as shown in (18).

$$\begin{cases}\frac{\partial L(\beta',\theta,d,\mu,\lambda)}{\partial\theta}=0\\ \frac{\partial L(\beta',\theta,d,\mu,\lambda)}{\partial\beta'}=0\end{cases} \quad (18)$$

From (18), the expression of the clock offset can be obtained by differentiating the logarithm of (7) and setting the result to zero.

$$\frac{\partial L(\beta',\theta,d,\lambda)}{\partial\theta}=-\frac{3}{2}\sum_{i=1}^{N}\left[\frac{-\beta'}{\beta'(T_{2,i}-\theta)-T_{1,i}-d}+\frac{\beta'}{T_{4,i}-d-\beta'(T_{3,i}-\theta)}\right] \quad (19)$$

The estimated clock offset $\hat{\theta}$ is expressed in (20).

$$\hat{\theta}=\frac{\sum_{i=1}^{N}\left[\beta'\left(T_{2,i}+T_{3,i}\right)-\left(T_{1,i}+T_{4,i}\right)\right]}{2N\beta'} \quad (20)$$

Similarly, we can obtain the expression of $\hat{\beta}'$ by differentiating the logarithm of (7) and setting the result to zero.

$$\frac{\partial L(\beta',\theta,d,\lambda)}{\partial \beta'} = -\frac{3}{2}\sum_{i=1}^{N}\left[\frac{T_{2,i}-\theta}{\beta'(T_{2,i}-\theta)-T_{1,i}-d} - \frac{T_{3,i}-\theta}{T_{4,i}-d-\beta'(T_{3,i}-\theta)}\right] - \frac{\lambda}{2\mu^2}\sum_{i=1}^{N}(T_{2,i}-T_{3,i}) \quad (21)$$

$\hat{\beta}'$ can be expressed as

$$\hat{\beta}' = \frac{\sum_{i=1}^{N}(T_{3,i}-T_{2,i})[(T_{2,i}-\theta)(T_{4,i}-d)+(T_{3,i}-\theta)(T_{1,i}+d)]+2\frac{3\mu^2}{\lambda}\sum_{i=1}^{N}(T_{3,i}-\theta)(T_{2,i}-\theta)}{2\sum_{i=1}^{N}(T_{3,i}-T_{2,i})(T_{2,i}-\theta)(T_{3,i}-\theta)} \quad (22)$$

Since $\beta' = \frac{1}{\beta}$, the estimated clock skew $\hat{\beta}$ can be given as:

$$\hat{\beta} = \frac{2\sum_{i=1}^{N}(T_{3,i}-T_{2,i})(T_{2,i}-\theta)(T_{3,i}-\theta)}{\sum_{i=1}^{N}(T_{3,i}-T_{2,i})[(T_{2,i}-\theta)(T_{4,i}-d)+(T_{3,i}-\theta)(T_{1,i}+d)]+2\frac{3\mu^2}{\lambda}\sum_{i=1}^{N}(T_{3,i}-\theta)(T_{2,i}-\theta)} \quad (23)$$

We use the estimated $\hat{\lambda}, \hat{\mu}$ obtained in Section III-A and put (20) into (23). The estimated clock skew $\hat{\beta}$ can be expressed as (24).

$$\hat{\beta} = \frac{\sum_{i=1}^{N}(T_{2,i}+T_{3,i})\sum_{i=1}^{N}(T_{2,i}+T_{3,i})-4N\sum_{i=1}^{N}T_{2,i}T_{3,i}}{\sum_{i=1}^{N}(T_{1,i}+T_{4,i})\sum_{i=1}^{N}(T_{2,i}+T_{3,i})-2N\sum_{i=1}^{N}(T_{1,i}T_{2,i}+T_{3,i}T_{4,i}-d(T_{3,i}-T_{2,i}))} \quad (24)$$

The procedure of the entire proposed scheme can be summarized in Fig. 3.

IV. Analytical Analysis of Convergence

In this section, the mathematical analysis of the convergence is performed. The convergence of the clock offsets is expressed as following.

$$C_\theta = \lim_{N\to\infty}\left|\hat{\theta}_N - \hat{\theta}_{N-1}\right|$$

$$= \lim_{N\to\infty}\left|\frac{\sum_{i=1}^{N}[\beta'(T_{2,i}+T_{3,i})-(T_{1,i}+T_{4,i})]}{2N\beta'} - \frac{\sum_{i=1}^{N-1}[\beta'(T_{2,i}+T_{3,i})-(T_{1,i}+T_{4,i})]}{2(N-1)\beta'}\right|$$

$$= \lim_{N\to\infty}\left|\frac{(T_{2,N}+T_{3,N})-\beta(T_{1,N}+T_{4,N})}{2N(N-1)} - \frac{\sum_{i=1}^{N-1}[(T_{2,i}+T_{3,i})-\beta(T_{1,i}+T_{4,i})]}{2N(N-1)}\right| \quad (25)$$

Based on Section III(A), we assumes $|x_i - y_i| = \xi$. Then $\left|(T_{2,i}+T_{3,i}) - \beta(T_{1,i}+T_{4,i})\right| = \xi$. The limit C_θ can be expressed in (26).

$$C_\theta = \lim_{N\to\infty}\left|\frac{(T_{2,N}+T_{3,N})-\beta(T_{1,N}+T_{4,N})}{2N(N-1)} - \frac{\sum_{i=1}^{N-1}[(T_{2,i}+T_{3,i})-\beta(T_{1,i}+T_{4,i})]}{2N(N-1)}\right|$$

$$\le \lim_{N\to\infty}\left|\frac{(T_{2,N}+T_{3,N})-\beta(T_{1,N}+T_{4,N})}{2N(N-1)}\right| + \lim_{N\to\infty}\left|\frac{\sum_{i=1}^{N-1}[(T_{2,i}+T_{3,i})-\beta(T_{1,i}+T_{4,i})]}{2N(N-1)}\right|$$

$$= \lim_{N\to\infty}\left|\frac{\xi}{2N(N-1)}\right| + \lim_{N\to\infty}\left|\frac{(N-1)\xi}{2N(N-1)}\right| = \lim_{N\to\infty}\left|\frac{\xi}{2N}\right| \quad (26)$$

The order of the numerator is smaller than that of the denominator with respect to N. When N tends to infinite, we can get $C_\theta = 0$.

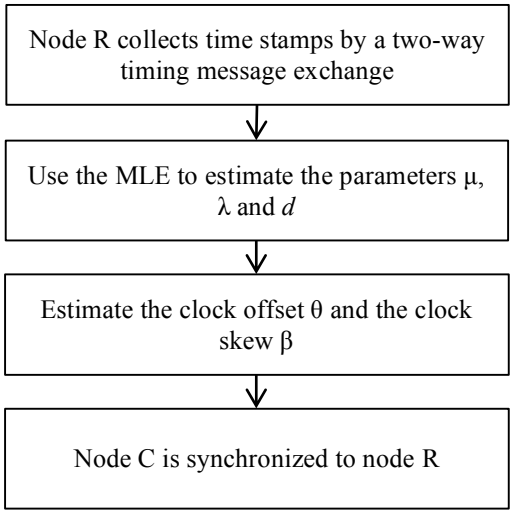

Fig. 3. Flowchart representation of the proposed scheme.

The convergence of the clock skew can be obtained by comparing the clock skews between the adjacent message exchanges.

$$C_\beta = \lim_{N\to\infty}\left(\frac{\hat{\beta}_N}{\hat{\beta}_{N-1}}\right)$$

$$= \lim_{N\to\infty}\left(\frac{2\sum_{i=1}^{N}(T_{2,i}-\theta)(T_{3,i}-\theta)}{\sum_{i=1}^{N}[(T_{2,i}-\theta)(T_{4,i}-d)+(T_{3,i}-\theta)(T_{1,i}+d)]} \times \frac{\sum_{i=1}^{N-1}[(T_{2,i}-\theta)(T_{4,i}-d)+(T_{3,i}-\theta)(T_{1,i}+d)]}{2\sum_{i=1}^{N-1}(T_{2,i}-\theta)(T_{3,i}-\theta)}\right)$$

$$= \lim_{N\to\infty}\left(\frac{1+\frac{(T_{2,N}-\theta)(T_{3,N}-\theta)}{\sum_{i=1}^{N-1}(T_{2,i}-\theta)(T_{3,i}-\theta)}}{1+\frac{(T_{2,N}-\theta)(T_{4,N}-d)+(T_{3,N}-\theta)(T_{1,N}+d)}{\sum_{i=1}^{N-1}[(T_{2,i}-\theta)(T_{4,i}-d)+(T_{3,i}-\theta)(T_{1,i}+d)]}}\right) = 1 \quad (27)$$

Based on the analytical analysis from (25) to (27), it is clear that the clock offset and the clock skew converge after N rounds of message exchanges.

V. Simulation Results and Discussions

In this section, numerical simulations in MATLAB are performed to validate the performances of our proposed solutions for clock synchronization. The simulation results are presented and discussed.

A. Selection of Parameters

The parameters used in the simulations are set as follows. The diffusion coefficient D is set to $1000\ \mathrm{nm}^2/\mu\mathrm{s}$, which is selected according to the diffusion coefficient of ionic calcium in cytoplasm [34]. The propagation distance between the transmitter and the receiver is set from 10 μm to 200 μm, which is a typical distance between two nanomachines as in [12]. The mean value μ and the scaling parameter λ of the inverse Gaussian distribution are set to $\mu \in [0, 1]$ and $\lambda \in [1, 5]$, respectively. The clock synchronization period and the fixed delay are usually at the order of millisecond (ms). The clock synchronization period is set to 10 ms. It indicates that the difference between $T_{1,i}$ and $T_{1,i+1}$ is 10 ms. The fixed

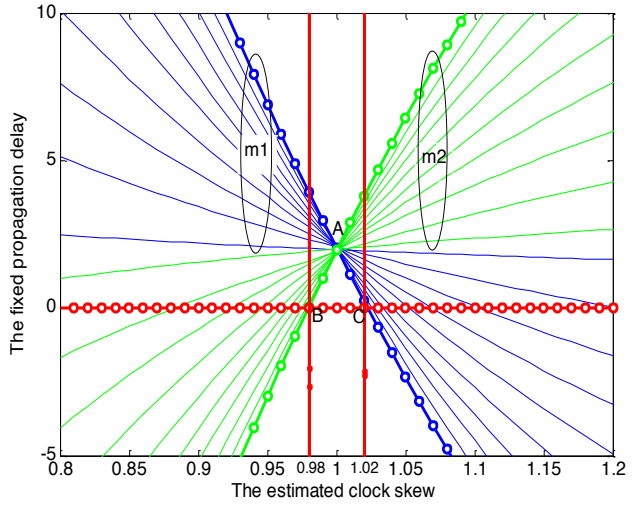

Fig. 4. The estimated feasible region for the clock skew $\hat{\beta}$ with N=10.

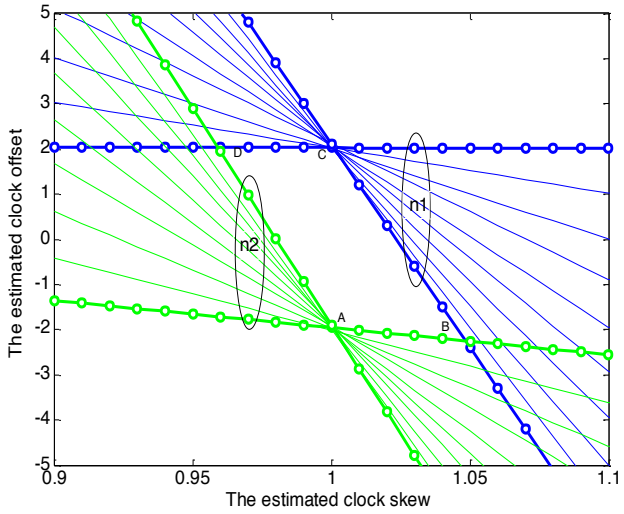

Fig. 5. The estimated clock offset $\hat{\theta}$ vs. the estimated clock skew $\hat{\beta}$ with N=10.

delay is assumed as a constant value for the same propagation distance. The clock offset θ and clock skew β are set to $\theta\epsilon(-2\ ms, 2\ ms)$ and $\beta\epsilon(0.98, 1.02)$, respectively. The above-mentioned parameters are given in Table I.

Table I. Simulation parameters

Parameters	Values
Diffusion coefficient	1000 nm²/μs
Propagation distance	10-200 μm
Mean of propagation delay $\boldsymbol{\mu}$	0-1
Scaling parameter $\boldsymbol{\lambda}$	1-5
Clock synchronization period	10 ms
Fixed delay	0.1-2 ms
Clock offset	-2-2 ms
Clock skew	0.98-1.02

B. Numerical Tests

The simulations are conducted to examine the performance of the estimators for the clock skew and the clock offset. The feasible region of the estimated clock skew is shown in Fig. 3. They are calculated by (17). This figure is for $N = 10$ and $\theta = 0$. The lines, enclosed in ellipse $\{m1\}$, are $\left\{\hat{d} = \frac{T_{2,i}-\theta}{\beta} - T_{1,i}\right\}_{i=1}^{N}$; the lines, enclosed in ellipse $\{m2\}$, are $\left\{\hat{d} = T_{4,i} - \frac{T_{3,i}-\theta}{\beta}\right\}_{i=1}^{N}$. The horizontal line is *d=0*. They form a common area $\{A, B, C\}$. The estimated clock skew is constrained by $\{A, B, C\}$. From Fig. 4, it is clear that the feasible region of the estimated clock skew is between 0.98 and 1.02, shown as the two vertical lines, which are the boundaries used for the simulation. This indicates that the estimated clock skews are valid. It demonstrates the effectiveness of our solution.

The feasible region of the estimated clock offset is shown in Fig. 5. Setting the fixed propagation delay $d \in (0, 2\ ms)$, we can numerically compute the feasible region of the estimated clock offset from (17). X - axis is the estimated clock skew and y-axis is the estimated clock offset. The lines, enclosed in the ellipse $\{n1\}$, are $\left\{\theta = T_{2,i} - \beta(T_{1,i} + \hat{d})\right\}_{i=1}^{N}$. The lines, enclosed in the ellipse $\{n2\}$, are $\left\{\theta = T_{3,i} - \beta(T_{4,i} - \hat{d})\right\}_{i=1}^{N}$. They form a common area $\{A, B, C, D\}$. The quadrilateral $\{A, B, C, D\}$ is the feasible region of the estimated clock offset. The figure shows that the feasible region is between -2 ms and 2 ms. The calculated $\hat{\theta}$ and $\hat{\beta}$ acquired by the MLE match the pre-defined parameters. This proves the validness of our solution.

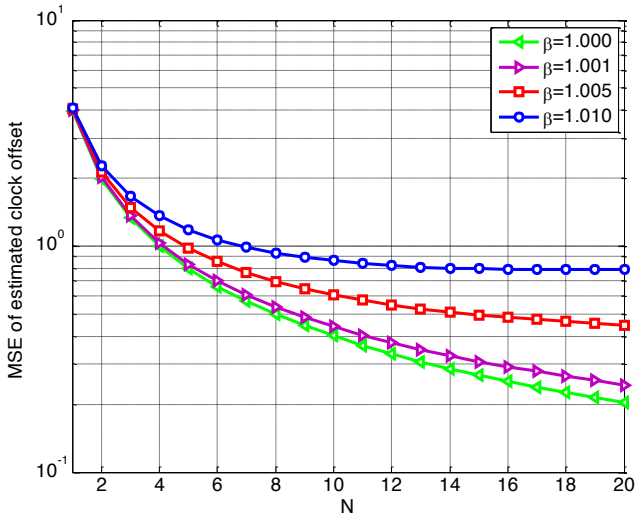

Fig. 6. The MSE of estimated clock offset with respect to the number of rounds of message exchange *N*.

Fig. 6 describes the mean square error (MSE) of the estimated clock offset versus the number of rounds of message exchanges. The initial clock offset is set to 2 ms and the initial clock skew is set to 1.000, 1.001, 1.005 and 1.010. The MSE of the estimated clock offset is numerically computed from (20). For the curves ($\beta = 1.000$, $\beta = 1.001$, $\beta = 1.005$, $\beta = 1.010$), it is clear that the MSE for the estimated clock offset $\hat{\theta}$ decreases and converges after a number of rounds of message exchanges. It demonstrates the effectiveness of the proposed estimator of the clock offset. From the figure it can also be seen

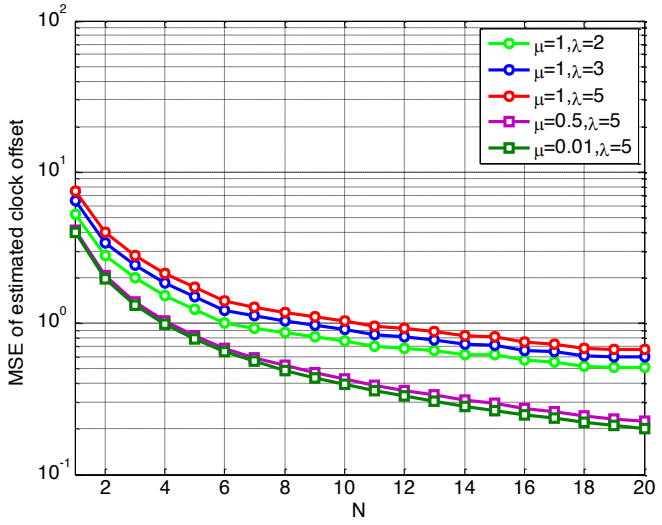

Fig. 7. The MSE of the estimated clock offset with μ and λ with respect to the number of rounds of message exchange N.

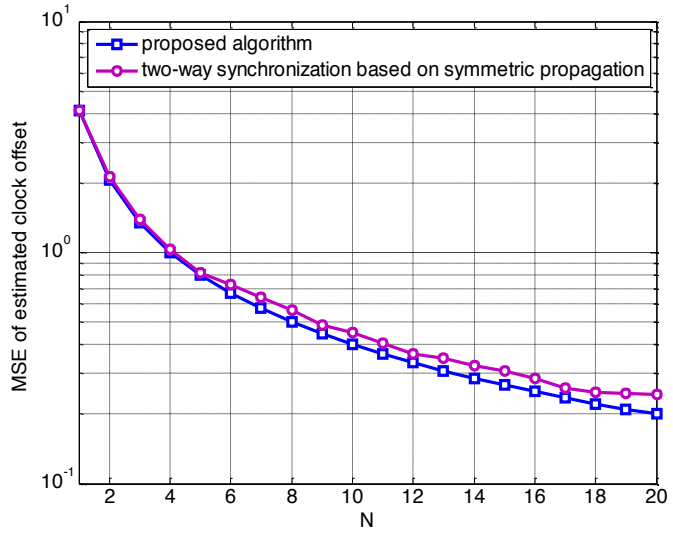

Fig. 8. The comparison of the proposed MLE and a synchronization method based on symmetrical propagation delay.

that different clock skews lead to different clock offsets. If the clock skew is larger, the MSE of the clock offset will be larger. Without clock skew error ($\beta = 1.000$), the MSE of the clock offset is smallest.

The MSE of the estimated clock offset versus N, given different μ and λ, is shown in Fig. 7. The initial clock offset is set to 2 ms. Each curve corresponds to a pair of $\{\lambda, \mu\}$. All the curves converge asymptotically to a constant. This proves the effectiveness of our MLE method. It can also be obtained that different $\{\lambda, \mu\}$ can lead to different MSEs of the estimated clock offsets. The bigger the scaling parameter λ is, the bigger the MSE of the estimated clock offset is. If the mean μ decreases, the MSE of the estimated clock offset decreases.

The MSEs of the estimated clock offset by the proposed MLE and a synchronization approach based on the symmetrical propagation delay are compared as shown in Fig. 8. Here the symmetrical propagation means that the delays from the transmitter nanomachine to the receiver nanomachine and from the receiver nanomachine to the transmitter nanomachine are

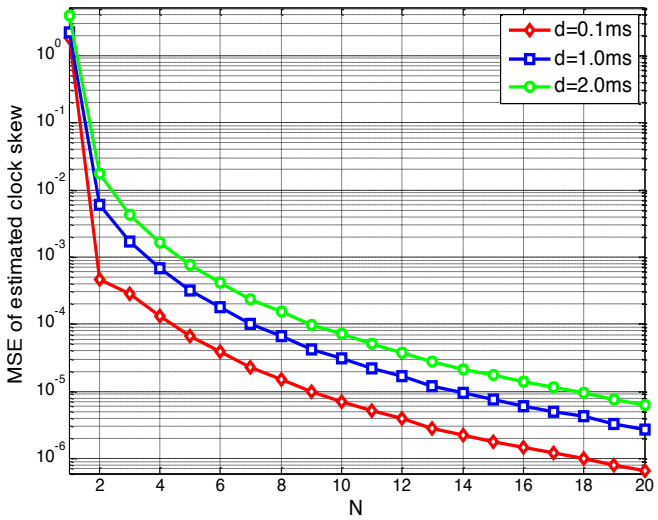

Fig. 9. The MSE of estimated clock skew with respect to the number of rounds of message exchange N.

the same. The initial clock offset is set to 2 ms and the initial clock skew is set to 1.001. The parameters used in these two scenarios including propagation distance, period, molecular concentration, and channel environment are all the same. From the figure, for both of the solutions, the MSEs of the estimated clock offset monotonically decrease and converge. It is obvious that our proposed clock synchronization solution can achieve a smaller clock offset than the other method. This demonstrates that the proposed MLE scheme has a better performance.

The MSE of the estimated clock skew versus N is shown in Fig. 9. It is numerically computed from (24). The fixed propagation delays are set to 0.1 ms, 1.0 ms and 2.0 ms. It is clearly shown in the figure the MSE of the estimated clock skew decreases and converges along with a number of two-way message exchanges. And different fixed propagation delays cause different MSEs of the estimated clock skew. A larger fixed delay d represents a larger distance. The larger the propagation distance is, the larger the fixed propagation delay is. The large fixed delay makes the recorded time stamps large and therefore large MSE of estimated clock skew.

A scenario of a nanonetwork with multiple nanomachines is also simulated. In the network, one reference node and M child nodes form a simple network in the star topology. For simplicity, we assume that the nanomachines only have offset errors without skew errors. Each child node would be synchronized with the reference node using the proposed MLE scheme in Section III. The performance of the clock synchronization for the network can be measured by the MSE of the offsets of the nanomachines as

$$\mathrm{MSE} = \frac{1}{\mathrm{M}} \sum_{\mathrm{i}=1}^{\mathrm{M}} \left(\hat{\theta}^{\mathrm{i}} - \theta^{\mathrm{i}} \right)^2 \tag{28}$$

where θ^i is the true clock offset between node i and the reference node, and $\hat{\theta}^i$ is the estimated clock offset. The initial clock offset between node i and the reference node is uniformly generated between 1 ms and 2 ms. Fig. 10 shows the relationship of the MSE for the clock synchronization with respect to the number of rounds of the message exchanges for

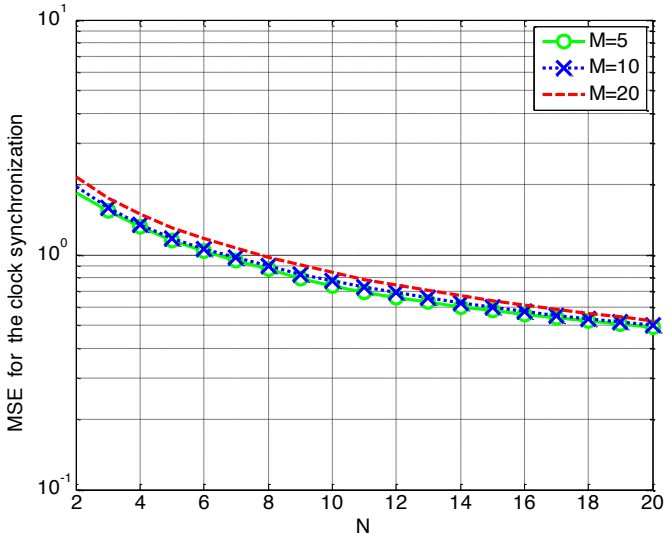

Fig. 10. The MSE for the clock synchronization with respect the number of rounds of message exchanges for different network sizes.

different network sizes. The MSE decreases as the increase of the number of the iterations, which proves the effectiveness of the proposed MLE scheme. It is also clear from the figure that the accuracy would become worse if the network size increases.

VI. Conclusion

In this paper, we have addressed the issue of the clock synchronization for the nanomachines working in the nanonetworks. The main purpose of this work is to estimate the clock offset and the clock skew for the clock synchronization, therefore enabling the nanomachines to work in an identical time frame. The two-way message exchange mechanism with the molecular propagation delay based on the inverse Gaussian distribution is modeled between a transmitter nanomachine and a receiver nanomachine. The clock offset and the clock skew have been estimated by the MLE. For evaluating the performance of our scheme, the MSEs of the estimated clock skews and the clock offsets have been simulated and compared with that of an existing scheme. The simulation results demonstrate that our proposed clock synchronization method can achieve a better performance.

Acknowledgment

This study has been sponsored by the Scientific Research Foundation for the Returned Overseas Chinese Scholars from State Education Ministry, the Shanghai Sailing Program from Science and Technology Commission of Shanghai Municipality (STCSM) under the grant No. 14YF1408700, the College & University Young Teachers' Training Program from Shanghai Municipal Education Commission, and Shanghai Key Laboratory of Power Station Automation Technology.

References

[1] I. F. Akyildiz, F. Brunetti, and C. Blázquez, "Nanonetworks: A new communication paradigm," *Comput. Netw.,* vol. 52, pp. 2260-2279, 2008.

[2] T. Nakano, M. J. Moore, F. Wei, A. V. Vasilakos, and J. Shuai, "Molecular communication and networking: Opportunities and challenges," *IEEE Trans. Nanobiosci.,* vol. 11, pp. 135-148, 2012.

[3] T. Nakano, T. Suda, Y. Okaie, M. Moore, and A. Vasilakos, "Molecular Communication Among Biological Nanomachines: A Layered Architecture and Research Issues," *IEEE Trans. Nanobiosci.,* vol. 13, pp. 169 - 197, 2014.

[4] L. Schenato and F. Fiorentin, "Average TimeSynch: A consensus-based protocol for clock synchronization in wireless sensor networks," *Automatica,* vol. 47, pp. 1878-1886, 2011.

[5] Q. Li and D. Rus, "Global clock synchronization in sensor networks," *IEEE Trans. Comput.,* vol. 55, pp. 214-226, 2006.

[6] S. Ganeriwal, R. Kumar, and M. B. Srivastava, "Timing-sync protocol for sensor networks," in *Proc. 1st Int. Conf. Embed. Netw. sensor Syst.*, New York, NY, 2003, pp. 138-149.

[7] M. Akhlaq and T. R. Sheltami, "RTSP: An Accurate and Energy-Efficient Protocol for Clock Synchronization in WSNs," *IEEE Trans. Instrum. Meas.,* vol. 62, pp. 578-589, 2013.

[8] E. Garone, A. Gasparri, and F. Lamonaca, "Clock synchronization for wireless sensor network with communication delay," in *American Control Conference (ACC)*, Washington, 2013, pp. 771-776.

[9] H. S. Abdel-Ghaffar, "Analysis of synchronization algorithms with time-out control over networks with exponentially symmetric delays," *IEEE Trans. Commun.,* vol. 50, pp. 1652-1661, 2002.

[10] X. Gang and K. Shalinee, "Analysis of distributed consensus time synchronization with Gaussian delay over wireless sensor networks," *EURASIP J. Wireless Commun. Netw.,* 2009:528161, 2009.

[11] K. Srinivas, A. W. Eckford, and R. S. Adve, "Molecular communication in fluid media: The additive inverse gaussian noise channel," *IEEE Trans. Inf. Theory,* vol. 58, pp. 4678-4692, 2012.

[12] R. Chhikara, *The Inverse Gaussian Distribution: Theory: Methodology, and Applications* vol. 95: CRC Press, 1988.

[13] M. Pierobon and I. F. Akyildiz, "A physical end-to-end model for molecular communication in nanonetworks," *IEEE J. Sel. Areas Commun.,* vol. 28, pp. 602-611, 2010.

[14] L. Hui, S. M. Moser, and G. Dongning, "Capacity of the Memoryless Additive Inverse Gaussian Noise Channel," *IEEE J. Sel. Areas Commun.,* vol. 32, pp. 2315-2329, 2014.

[15] A. Noel, K. C. Cheung, and R. Schober, "Improving receiver performance of diffusive molecular communication with enzymes," *IEEE Trans. Nanobiosci.,* vol. 13, pp. 31-43, 2014.

[16] M. Heinemann and S. Panke, "Synthetic biology—putting engineering into biology," *Bioinformatics,* vol. 22, pp. 2790-2799, 2006.

[17] J.-M. Fustin, M. Doi, Y. Yamaguchi, H. Hida, S. Nishimura, M. Yoshida, *et al.*, "RNA-methylation-dependent RNA processing controls the speed of the circadian clock," *Cell,* vol. 155, pp. 793-806, 2013.

[18] M. B. Elowitz and S. Leibler, "A synthetic oscillatory network of transcriptional regulators," *Nature,* vol. 403, pp. 335-338, 2000.

[19] R. Phillips, J. Kondev, J. Theriot, and H. Garcia, *Physical biology of the cell*: Garland Science, 2012.

[20] C. Lo, Y.-J. Liang, and K.-C. Chen, "A Phase Locked Loop for Molecular Communications and Computations," *IEEE J. Sel. Areas Commun.,* vol. 32, pp. 2381-2391, 2014.

[21] S. Abadal and I. F. Akyildiz, "Bio-Inspired Synchronization for Nanocommunication Networks," in *Proc. IEEE GLOBECOM*, 2011, pp. 1-5.

[22] S. Abadal and I. F. Akyildiz, "Automata modeling of quorum sensing for nanocommunication networks," *Nano Commun. Netw.,* vol. 2, pp. 74-83, 2011.

[23] M. J. Moore and T. Nakano, "Synchronization of inhibitory molecular spike oscillators," in *Bio-Inspired Models of Networks, Information, and Computing Systems*: Springer, 2012, pp. 183-195.

[24] M. J. Moore and T. Nakano, "Oscillation and Synchronization of Molecular Machines by the Diffusion of Inhibitory Molecules," *IEEE Trans. Nanotechnol.,* vol. 12, pp. 601-608, 2013.

[25] H. ShahMohammadian, G. G. Messier, and S. Magierowski, "Blind Synchronization in Diffusion-Based Molecular Communication Channels," *IEEE Commun. Lett.,* vol. 17, pp. 2156-2159, 2013.

[26] J. Philibert., "One and a half century of diffusion: Fick, Einstein, before and beyond," *Diffusion Fundamentals,* pp. 1-10, 2006.

[27] J. P. Rospars, V. Krivan, and P. Lansky, "Perireceptor and receptor events in olfaction. Comparison of concentration and flux detectors: a modeling study," *Chemical senses,* vol. 25, pp. 293-311, Jun 2000.

[28] M. Pierobon and I. F. Akyildiz, "Capacity of a diffusion-based molecular communication system with channel memory and molecular noise,"

IEEE Trans. Inf. Theory, vol. 59, pp. 942-954, 2013.
[29] N.-R. Kim and C.-B. Chae, "Novel modulation techniques using isomers as messenger molecules for nano communication networks via diffusion," *IEEE J. Sel. Areas Commun.,* vol. 31, pp. 847-856, 2013.
[30] E. L. Cussler, "Diffusion. Mass Transfer in Fluid Systems," *Cambridge University Press,* vol. 2nd edition, 1997.
[31] D. L. Mills, "Internet time synchronization: the network time protocol," *IEEE Trans. Commun.,* vol. 39, pp. 1482-1493, 1991.
[32] J. Devore, "Probability and Statistics for Engineering and the Sciences," *Cengage Learning,* 2011.
[33] S. A. Murphy and A. W. Van der Vaart, "On profile likelihood," *Journal of the American Statistical Association,* vol. 95, pp. 449-465, 2000.
[34] Brian S. Donahue and R. F. Abercrombie, "Free diffusion coefficient of ionic calcium in cytoplasm," *Cell Calcium,* vol. 8, pp. 437-448, Dec 1987.